Realizing negative Poisson's ratio in spring networks with close-packed lattice geometries

Jun Liu,[1] Yunhuan Nie,[1] Hua Tong,[2] and Ning Xu[1,*]

[1]*Hefei National Laboratory for Physical Sciences at the Microscale, CAS Key Laboratory of Soft Matter Chemistry, and Department of Physics, University of Science and Technology of China, Hefei 230026, People's Republic of China*

[2]*Department of Fundamental Engineering, Institute of Industrial Science, University of Tokyo, 4-6-1 Komaba, Meguro-ku, Tokyo 153-8505, Japan*

(Received 25 October 2018; published 24 May 2019)

Previously, auxetic materials were realized by designing building blocks with specific geometries or tuning topology of spring networks. Here, we propose a new approach by properly manipulating the disorder, especially the bond stiffness disorder, of an unstressed spring network. When randomly distorting a spring network initially with a close-packed lattice structure, we find that the resultant unstressed network becomes auxetic. Resulted from the distortion, longer bonds are likely to contribute more to the shear modulus but less to the bulk modulus. Inspired by this correlation, we realize isotropic auxeticity in the unstressed triangular lattice, by distributing each bond a spring constant according to a virtual lattice distortion. In the perspective of previous approaches, however, it is not straightforward to figure out how the close-packed lattices can be turned into auxetic independent of directions. The key of our approach is the correlated disorder induced by the (virtual) lattice distortion, which leads to a sufficiently large nonaffine contribution responsible to the auxeticity.

DOI: 10.1103/PhysRevMaterials.3.055607

I. INTRODUCTION

When an elastic material is stretched or compressed in one direction by a strain of $\epsilon_{\parallel}$, it deforms in the perpendicular direction by a strain of $\epsilon_{\perp}$. This elastic property can be quantified by the Poisson's ratio, $\nu = -d\epsilon_{\perp}/d\epsilon_{\parallel}$ [1]. Intuitively, normal elastic materials should have a positive Poisson's ratio. For example, a rubber band becomes thinner when being stretched. However, some man-made materials expand (shrink) upon stretch (compression) and thus have a negative Poisson's ratio [2–18]. These special functional materials are named as auxetic materials [4], a typical type of mechanical metamaterials with important applications [5,16–18].

In many of the previous studies, auxeticity has been realized by the design of building blocks with special geometries, e.g., reentrant structures [2,4], hinged rotating rigid polygons [11], folded and pleated structures [8,9], etc. Modern low-dimensional functional materials such as carbon nanotube sheets [13], graphene-based materials [12], and black phosphorus [7] can also exhibit auxeticity under certain conditions, but are still attributed to micro-structural origins. Moreover, auxetic behaviors have been observed in some bulk crystals like cubic metals [19], alloys [20], and quartz [21], but only in specific directions due to simple geometric reasons. It seems that selected local geometries are crucial for the occurrence of the negative Poisson's ratio. In pure geometric perspective, two-dimensional triangular lattice cannot be auxetic; though auxetic in certain directions, three-dimensional close-packed cubic lattices are unexpected to be auxetic in arbitrary directions, either. Therefore close-packed lattices seem not possess local geometries favorable to auxeticity. In this work, we aim at finding a general approach to achieve auxetic materials, which is not picky to building blocks with specific geometries. If such an approach exists, we would expect to turn close-packed lattices into auxetic.

Some recent studies have indeed proposed an alternate way to obtain auxetic materials by selectively altering the topology of unstressed disordered solids [22–27]. Unlike crystalline lattices which are anisotropic, disordered solids are isotropic. There is also no apparent microscopic building blocks in disordered solids. Otherwise, the nature of disordered solids would not be so elusive. For isotropic materials, the Poisson's ratio can be expressed in terms of elastic moduli [5]: $\nu_{\rm isot} = \frac{d-2G/B}{d(d-1)+2G/B}$, with d, G, and B being the dimension of space, shear modulus, and bulk modulus, respectively. In order to realize the negative Poisson's ratio, the material is required to have a large enough $G/B(>d/2)$. This provides a way to design auxetic materials by tuning material's elastic moduli, although it is challenging and even counter-intuitive to have isotropic materials to be rigid to shear but vulnerable to compression. It has been found that, at the bond level, responses to compression and shear in disordered solids are independent of each other, so that the negative Poisson's ratio can be realized by selectively pruning bonds [22]. Intuitively, cutting bonds will change elastic properties of close-packed lattices. However, for a perfect close-packed lattice with identical bonds, which bonds should be selected to remove? One may then come up with the idea of removing bonds randomly. As will be shown later, it does not work to decrease the Poisson's ratio. Therefore this pruning-bond approach is not the one that we look for.

*ningxu@ustc.edu.cn

In both of the previous approaches, the influence of the bond stiffness has been omitted. Note that the spatial variation or disorder of the bond stiffness can also affect the elastic properties of close-packed lattices and make the lattices isotropic. In this work, surprisingly we find that the bond stiffness disorder is actually the right element to induce isotropic auxeticity in close-packed lattices. However, the disorder needs to be introduced following a hidden rule. A totally random introduction of the disorder cannot work. The breakthrough comes from our finding that randomly distorting the close-packed lattices can lead to auxeticity and a special correlation between elastic moduli and bond length: statistically, longer bonds contribute more to the shear modulus but less to the bulk modulus. Inspired by this correlation, we develop the rule to manipulate the bond stiffness disorder. That is to assume a virtual lattice distortion and distribute each bond a spring constant according to its virtual length. This significantly decreases the Poisson's ratio of close-packed lattices and even push it below zero. Therefore our work reveals another approach to design auxetic materials by manipulating the lattice site structural disorder or bond stiffness disorder, in which the lattice distortion plays the key role.

II. METHODS

We study two- and three-dimensional systems with periodic boundary conditions in all directions. The systems are initially perfect close-packed lattices with nearest lattice sites (nodes) being connected by relaxed springs of length l_0. There are totally N nodes in the system. Network distortion is performed by randomly displacing node i from crystalline lattice site $\vec{r}_{i,c}$ to $\vec{r}_i = \vec{r}_{i,c} + \vec{\eta}_i$. In two dimensions, $\vec{\eta}_i = (\eta\cos\theta_i, \eta\sin\theta_i)$ with θ_i being a random angle ranging from 0 to 2π. In three dimensions, $\vec{\eta}_i$ is randomly chosen from vectors uniformly distributed on a sphere of radius η centered at the origin. We set $\eta \leqslant l_0/2$ in order to avoid crossing of springs. The topology of the network, i.e., number of springs and their connections, remain unchanged after the distortion. To maintain mechanical stability, all networks concerned are unstressed with all springs being relaxed. Normally, a larger η causes a stronger structural disorder.

The elastic moduli and Poisson's ratio are obtained by slightly deforming the unstressed networks and calculating the linear response after the energy minimization [28]. Upon deformation, the energy stored in the spring connecting nodes i and j is

$$U_{ij} = \tfrac{1}{2}k(r_{ij} - l_{ij})^2, \tag{1}$$

where k is the spring constant, r_{ij} is the separation between nodes (i.e., length of the spring upon deformation), and l_{ij} is the length of relaxed spring before deformation. We set the crystalline lattice constant l_0 to be one.

Because our networks are unstressed, we apply a small compressive strain $\epsilon_\parallel$ in the x direction and minimize the energy while maintaining zero pressure in the perpendicular direction(s). The network responds to the compression by a deformation strain $\epsilon_\perp$ in the perpendicular direction(s). As long as $\epsilon_\parallel$ is small, we can always obtain a linear response, from which we determine the Poisson's ratio $\nu = -d\epsilon_\perp/d\epsilon_\parallel$.

III. RESULTS

A. Auxeticity by lattice distortion

In this part of the work, all springs always have the same spring constant (bond stiffness) $k = 1$. Figure 1 shows results of spring networks distorted from a two-dimensional triangular lattice. In such networks, each node is connected by six springs, so the average coordination number z is equal to 6, well above the isostatic value $z_{\rm iso} = 2d = 4$. This guarantees the mechanical stability and the rigidity of the unstressed spring networks [29–36].

Figure 1(a) compares the bulk and shear moduli, B and G. Although the triangular lattice is anisotropic, the shear modulus calculated from the simple shear is equal to that from the pure shear, so we do not need to worry about the variation of the shear modulus due to the way to impose shear. With the increase of η and hence the structural disorder, the system is more and more isotropic, as long as the system is large enough. This is also true when the bond stiffness disorder is introduced to the lattices, as will be shown later. The data collapse of $N = 1024$ and 16 384 systems shown in Fig. 1(a) confirms that our results do not rely on system size for sufficiently large systems in which the anisotropy can be avoided (we will discuss the results in the small system size limit later). Both G and B decrease when η increases. Apparently, B decays more quickly than G. Surprisingly, $G = B$ at a critical value of the distortion, $\eta_c \approx 0.446$. When $\eta > \eta_c$, B is even smaller than G. From the expression of the Poisson's ratio $\nu_{\rm isot}$ for isotropic materials shown in Sec. I, negative Poisson's ratio is expected at $\eta > \eta_c$.

As shown in Fig. 1(b), the Poisson's ratio ν decreases when η increases, which becomes negative when $\eta > \eta_c$. We also show $\nu_{\rm isot}$ for comparison, which collapses well with ν.

Since the negative Poisson's ratio emerges when η is large, disorder is likely to be the cause of auxetic networks. There are different ways to introduce disorder to a crystalline lattice, e.g., randomly distorting nodes as done here, removing bonds,

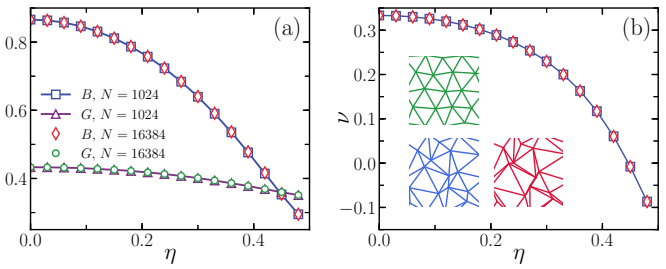

FIG. 1. Elastic properties subject to the network distortion from a two-dimensional triangular lattice with all springs having the same stiffness. (a) and (b) show the shear and bulk moduli, G and B, and the Poisson's ratio ν against the magnitude of the node displacement η, respectively. $\eta = 0$ corresponds to a perfect triangular lattice. Squares and diamonds in (b) are $\nu(\eta)$ and $\nu_{\rm isot}(\eta)$, respectively, as defined in the text, for $N = 1024$ systems. The lines are guides for the eye. The insets of (b) are a part of the networks at $\eta = 0.1$ (top), 0.3 (left bottom), and 0.46 (right bottom). The Poisson's ratio becomes negative when $\eta > 0.446$.

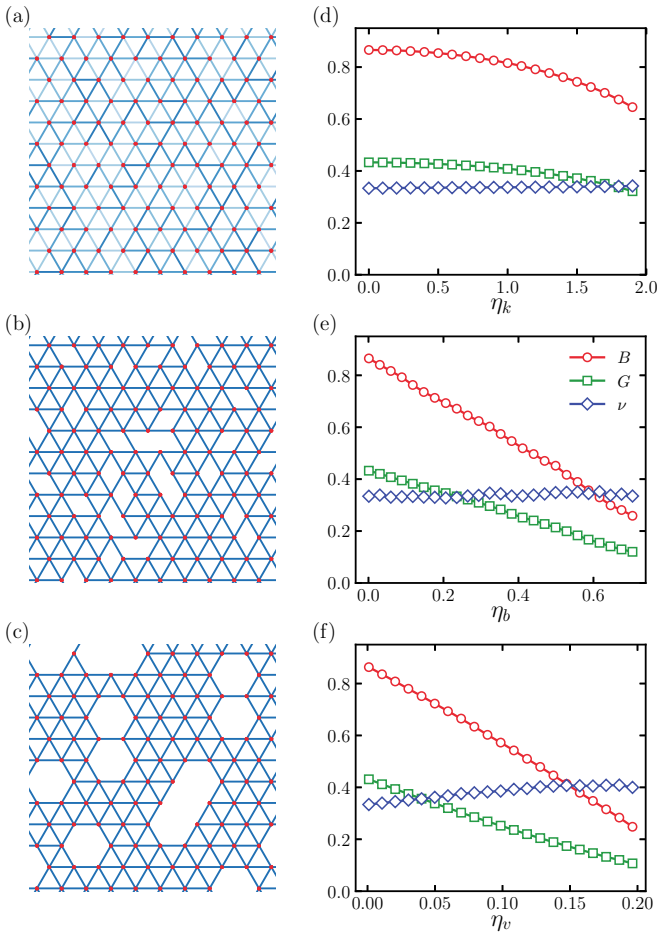

FIG. 2. Comparison of elastic properties subject to the increase of different types of disorder starting from a perfect triangular lattice with $N = 1024$ nodes. (a), (b), and (c) show a part of the systems with bond stiffness being varied (quantified by the gray scale of the bond), bonds being removed, and nodes being removed, respectively. (d), (e), and (f) show the corresponding bulk modulus B (circles), shear modulus G (squares), and Poisson's ratio ν (diamonds) as a function of the strength of disorder for the three cases in (a), (b), and (c), respectively. Here, η_k sets the range of the bond stiffness from $1 - \eta_k/2$ to $1 + \eta_k/2$, and η_b and η_v are respectively the fraction of bonds and nodes being randomly removed. In contrast to Fig. 1(b), the Poisson's ratios of the three cases do not decrease with the increase of the disorder.

removing nodes, or varying the bond stiffness [34]. However, as shown in Figs. 1 and 2, we only obtain negative ν by distorting nodes. In the other three ways, the Poisson's ratio does not tend to decrease upon the increase of disorder. The direct consequence of distorting nodes is the cause of bond length disorder. Note that each bond length is determined by the locations of two nodes. Therefore the bond length disorder caused by the lattice distortion correlates the displacements of adjacent nodes and is thus not totally random. For the other three types of disorder shown in Fig. 2, the change of any single bond or node is independent. This distinction suggests that the disorder needs to be introduced in some correlated rather than a totally random way, while distorting nodes happens to create this correlation.

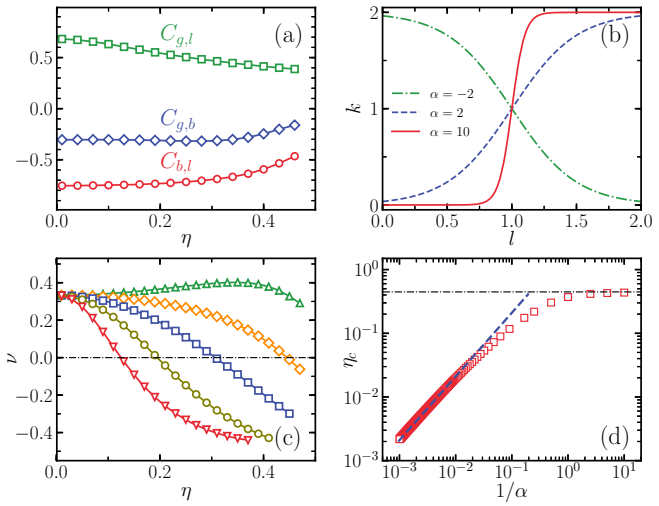

FIG. 3. Effects of the bond stiffness disorder on elastic properties of the networks. (a) Correlation functions $C_{g,l}$, $C_{g,b}$, and $C_{b,l}$ as defined in the text against the magnitude of the node displacement η for two-dimensional systems distorted from a triangular lattice with $N = 4096$. (b) Examples of spring constant function $k(l) = 1 + \tanh[\alpha(l - l_0)]$ with $l_0 = 1$ being the unit of length. (c) Poisson's ratio ν against η when spring constants are set by $k(l)$. From left to right, $\alpha = 10$ (down triangles), 5 (circles), 2 (squares), 0 (diamonds), and -2 (up triangles). The solid lines are guides for the eye. The horizontal dot-dashed line labels $\nu = 0$. (d) Correlation between η_c, the critical value of η at which $\nu = 0$, and α^{-1}. The dashed line shows the linear relation $\eta_c \sim \alpha^{-1}$ in the large α limit. The horizontal dot-dashed line labels the upper bound $\eta_c \approx 0.446$ when $\alpha = 0$.

B. Correlation between elastic moduli and spring length

Inspired by the approach of decomposing elastic moduli into bonds: $G = \sum_i g_i$ and $B = \sum_i b_i$ with the sums being over all bonds [22], we calculate g_i and b_i, the contributions of spring i to the shear and bulk moduli, for all $3N$ springs of the distorted triangular lattice. Figure 3(a) shows that $C_{g,b} = \langle \delta g \delta b \rangle = \langle (g - \bar{g})(b - \bar{b}) \rangle < 0$ when $\eta > 0$, where $\bar{g} = G/3N$, $\bar{b} = B/3N$, and $\langle \cdot \rangle$ denotes the average over springs and configurations. Therefore δg and δb are negatively correlated, indicating that a spring which helps to strengthen G tends to weaken B. Figure 3(a) also shows that $C_{g,l} = \langle \delta g \delta l \rangle > 0$ and $C_{b,l} = \langle \delta b \delta l \rangle < 0$, where $\delta l = l - \bar{l}$ with l and $\bar{l}$ being the spring length and its average value. Therefore longer springs ($l > \bar{l}$) tend to have a larger g and a smaller b.

This finding is rather inspiring. Up to now, all springs are set to have identical spring constant. If we make longer springs stiffer and shorter ones softer, we may be able to enhance G and meanwhile weaken B, so that the Poisson's ratio may become negative at smaller η.

C. Auxeticity by bond stiffness disorder determined by lattice distortion

We then let the bond stiffness k be an increase function of spring length l. By employing various functional forms of $k(l)$, we find that such manipulation of k indeed significantly decreases the Poisson's ratio. Here we present results

for a chosen form $k(l) = 1 + \tanh[\alpha(l - l_0)]$, where α sets the steepness of $k(l)$ in the vicinity of the triangular lattice constant l_0. As shown in Fig. 3(b), $k(l)$ is bounded in [0,2]. The results in Fig. 1 are just for the special case of $\alpha = 0$. We choose the above function for $k(l)$ just in order to let $k(l)$ be symmetrically distributed around the average value of 1, without other special reasons. We also repeat the calculations using the error function $k(l) = 1 + \mathrm{erf}[\alpha(l - l_0)]$ and find qualitatively similar results (not shown here).

For a given α, we distort the perfect triangular lattice as done above for $\alpha = 0$ and simultaneously distribute each spring a spring constant $k(l)$. For all $\alpha > 0$, Fig. 3(c) shows that $\nu(\eta)$ behaves similarly to the $\alpha = 0$ case. Interestingly, the critical value of the distortion η_c at which $\nu = 0$ decreases with the increase of α. The involvement of the bond stiffness disorder associated with the bond length greatly weakens the required lattice distortion for auxetic networks to occur. For comparison, we also show in Fig. 3(c) an example with $\alpha < 0$. As expected, negative α hinders the decrease of ν and pushes η_c to higher values. With sufficiently large values of $|\alpha|$, ν even grows with η. By forcing longer springs to be softer, we instead are able to achieve much larger ν than that of perfect crystalline lattice. The manipulation of α thus offers us the freedom to control the elastic moduli and the Poisson's ratio purposely.

Figure 3(d) shows how η_c varies with α. As mentioned above, when $\alpha = 0$, $\eta_c \approx 0.446$, which sets the upper bound of η_c purely induced by the lattice distortion without the help of the bond stiffness disorder. When α is large, Fig. 3(d) indicates that $\eta_c \sim \alpha^{-1}$. The negative Poisson's ratio is then mostly contributed by the bond stiffness disorder, because the lattice distortion is too small to cause significant change of ν on its own, as shown by curves in Fig. 1 in the $\eta \to 0$ limit. The lattice distortion just acts to provide a way to cause some spatially correlated bond stiffness distribution. The linear relation between η_c and α^{-1} indicates that, when the bond stiffness disorder dominates, the lattice distortion must lead to a bond length distribution wider than α^{-1} in order for auxetic networks to occur. When α is small, both the lattice distortion and the bond stiffness disorder contribute to the formation of auxetic networks, so $\eta_c(\alpha^{-1})$ deviates from the linear relation and approaches the upper limit gradually.

D. Auxeticity in triangular lattice without distortion

Figure 3(d) suggests that negative Poisson's ratio is possible in perfect triangular lattice geometry, if we are able to perform an $\eta \to 0$ distortion and set the spring constants to be either 2 or 0, because $\alpha \to \infty$. This suggests that auxetic networks can also be produced by removing bonds of a perfect lattice following the $\eta \to 0$ distortion, as long as the resultant network is still rigid. In this limit, the initial topology will be broken and half of the bonds will be removed. Therefore, as will be shown later, the system will indeed lose the rigidity because of the floppy modes. Next, however, we will show that there is a scheme to realize the negative Poisson's ratio in the $\eta = 0$ networks without having to destroy the lattice topology and lose the rigidity.

An interesting and inspiring result shown in Fig. 3(d) is that $\alpha \sim \eta_c^{-1}$ when α is large. Note that here η_c corresponds

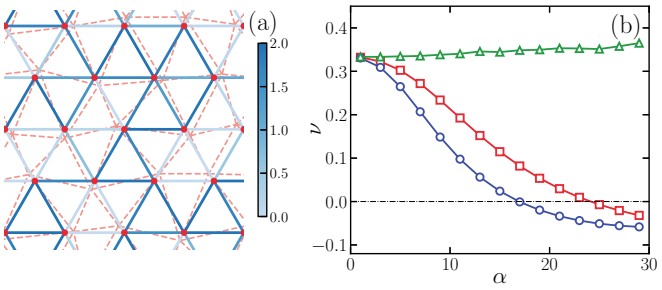

FIG. 4. Elastic properties of the triangular lattice without distortion and with the bond stiffness disorder being introduced by the virtual distortion. (a) Illustration of a part of a triangular lattice (solid) and its virtual distortion (dashed). The gray scale of the solid lines shows the value of the bond stiffness determined by the virtual distortion ($\eta^* = 0.15$ and $\alpha = 10$), as quantified by the scale bar. (b) Poisson's ratio ν against α for the $N = 16\,384$ triangular lattices. Spring constants are set by a virtual distortion of $\eta^* = 0.1$ (squares) and 0.15 (circles). The triangles show the case when spring constants set by $\eta^* = 0.15$ are randomly distributed to bonds, for comparison. The solid lines are guides for the eye. The horizontal dot-dashed line labels $\nu = 0$.

to a real lattice distortion. If we instead assume a virtual distortion η^* to a perfect lattice and distribute each bond a spring constant $k(l^*)$ with l^* being the virtual length of the bond after the virtual distortion, as illustrated by Fig. 4(a), can we achieve auxetic networks with finite α without any lattice distortion?

Figure 4(b) shows that the virtual distortion scheme indeed works. At fixed η^*, ν decreases with the increase of α and even drops below zero. With a larger η^*, a smaller α is required to obtain the negative Poisson's ratio. Different from previous approaches, auxetic materials are obtained here without designing any specific building blocks (microstructures) or destroying network topology, but just by utilizing the bond stiffness disorder.

To highlight the importance of the spatially correlated bond stiffness distribution generated by the lattice distortion, we show in Fig. 4(b) another $\nu(\alpha)$ curve obtained by randomly distributing the same set of spring constants from the virtual distortion. In sharp contrast, the Poisson's ratio does not decay with the increase of α any more. We realize the negative Poisson's ratio in the triangular lattice without distortion because of the finding of the crucial role of the lattice distortion in the cause of correlated disorder.

One may notice from Fig. 4(a) that there are some bonds which are so soft that they appear as if pruned. In Fig. 5(a), we show an example of the integrated bond stiffness distribution $I(k) = \int_0^k P_k(k')dk'$ for the case of $\eta^* = 0.15$ and $\alpha = 20$ with a negative Poisson's ratio, where $P_k(k')$ is the bond stiffness distribution. The bond stiffness of the weakest bonds is in the order of 10^{-5}, so it may not be necessary to keep such weak bonds there.

We then simply remove the weak bonds one by one in the sequence of increasing stiffness. However, with more and more bonds being removed, the system has to face to the danger of losing rigidity. Figure 5(b) shows the number of nontrivial floppy modes (i.e., normal modes of vibration

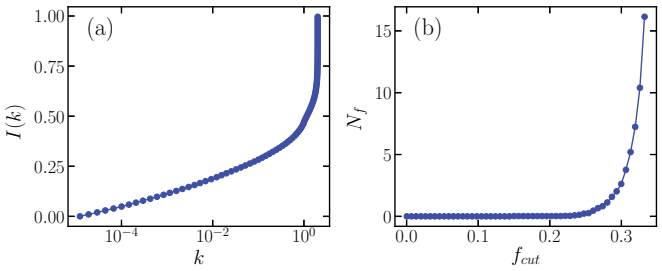

FIG. 5. Effects of removing weak bonds. (a) Integrated distribution of the bond stiffness, $I(k)$, for the triangular lattice with $N = 1024$ at $\alpha = 20$ and $\eta^* = 0.15$. Seen from Fig. 4(b), the Poisson's ratio is negative. (b) Number of nontrivial floppy modes, N_f, as a function of the fraction of bonds being removed, $f_{\rm cut}$. The bonds are removed in sequence of increasing stiffness. Nontrivial floppy modes emerge when $f_{\rm cut}$ is approximately above 0.25.

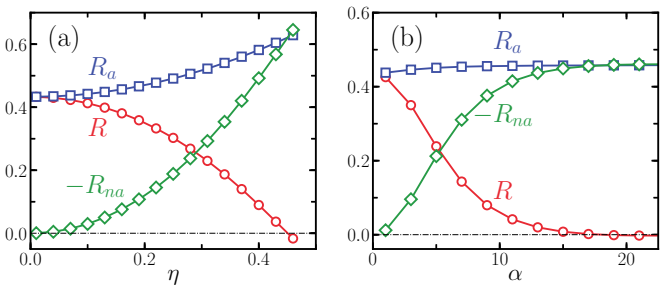

FIG. 6. Comparison of the total response R and its affine and nonaffine components R_a and R_{na} as defined in the text. R_{na} is always negative. In order to quantitatively compare it with R_a, which is positive, here we show $-R_{na}$. (a) and (b) are for the cases shown in Figs. 1(b) and 4(b) ($\eta^* = 0.15$), respectively. The horizontal dot-dashed lines label $R = 0$.

with a zero frequency, which do not consume energy), N_f, against the fraction of bonds being removed, $f_{\rm cut}$. The normal modes of vibration are obtained from the diagonalization of the Hessian matrix. Here, we only consider the floppy modes of nontrivial collective motion of nodes. The trivial zero-frequency modes caused by the periodic boundary conditions and by the nodes with only 0 or 1 bond left are excluded. The existence of nontrivial floppy modes indicates that the system loses its rigidity and cannot resist loads. Seen from Fig. 5(b), floppy modes emerge when $f_{\rm cut}$ reaches about 0.25, so we can cut at most 25% of the bonds. Therefore, in the $\alpha \to \infty$ limit when half of the bonds being removed, as discussed in the beginning of this section, the system can not be rigid.

It is thus important to use a finite α in order to maintain the rigidity of the networks. When the virtual distortion η^* is fixed, seen from the shape of $k(l^*)$ in Fig. 3(b), there are more and more weak bonds approaching the $k \to 0$ limit with the increase of α. Though weak, those bonds are still good for the network rigidity, as long as their stiffness is not negligible. For the case shown in Fig. 5, around $f_{\rm cut} = 0.25$ when the system loses the rigidity, the bond stiffness is already in the order of 0.01. Those bonds are stiff enough to affect the elastic properties of the networks and should not be simply removed. Therefore the cases shown here are still far away from the large α limit, where the stiffness of most of the bonds can be treated as either 0 or 2. An appropriate α leads to a number of bonds with stiffness distinct from 0 and 2, which are responsible to the auxeticity and the network rigidity.

E. Nonaffine contribution

We have seen that disorder is here the cause of auxetic networks, although it is not introduced in a totally random way. To understand the underlying mechanisms of such auxeticity, we may start with some unique properties induced by disorder. One direct consequence of disorder is the nonaffine deformation subject to strain [37–40]. In order to quantify the effects of nonaffinity, we calculate $R = dP_\perp/d\epsilon_\parallel$ and decompose it into an affine part R_a and a nonaffine part R_{na} [37–40], where $P_\perp$ is the pressure in the y direction induced by the strain $\epsilon_\parallel$ in the x direction. For two-dimensional networks,

$$R = R_a + R_{na} = -\frac{1}{A}\frac{\partial^2 U}{\partial\epsilon_\parallel \partial\epsilon_\perp} - \frac{1}{A}\sum_i \frac{\partial^2 U}{\partial\epsilon_\parallel \partial\vec{r}_i}\cdot\frac{d\vec{r}_i}{d\epsilon_\perp}, \quad (2)$$

where U is the total potential energy, A is the area of the system, and the sum is over all nodes. R_{na} can be calculated from the inverse of the Hessian matrix [37–40]. Apparently, R is negative when $\nu < 0$.

In Fig. 6, we compare R, R_a, and R_{na} for the $\alpha = 0$ and $\eta = 0$ ($\eta^* = 0.15$) cases of manipulating the triangular lattice. The affine component R_a is always positive and does not decay with the increase of η or α, which is apparently harmful to the formation of negative ν. In contrast, R_{na} is negative, whose absolute value increases when η or α increases and eventually beats R_a. Therefore nonaffinity induced by disorder is responsible to the formation of auxetic networks. However, nonaffinity is ubiquitous in disordered solids, while most of disordered solids do not have negative Poisson's ratio. The way that we produce auxetic networks happens to generate some elusive mechanisms to boost the contribution of nonaffinity, which should be different from normal disordered solids and calls for future studies.

F. Building blocks to form periodic mechanical metamaterials

In all the above simulations, we have deliberately focused on large systems, which tend to be isotropic when disorder is sufficiently large. In fact, any of the large auxetic networks shown above can be building blocks to form a periodic auxetic materials. However, in practice, we always expect that the building blocks are as simple as possible. It is then necessary to know how small the system can be to exhibit auxeticity.

The triangular lattice concerned here contains $\sqrt{N}$ nodes per row in both x and y directions. $\sqrt{N}$ needs to be even. Otherwise, the lattice structure will be broken in the y direction due to the periodic boundary conditions. The smallest system contains two nodes in each direction. However, under periodic boundary conditions, each node is connected with its nearest neighbors and their images, which seems unphysical. Therefore, the smallest systems concerned here should be $N = 16$. In fact, regardless of the illness of the $N = 4$ systems,

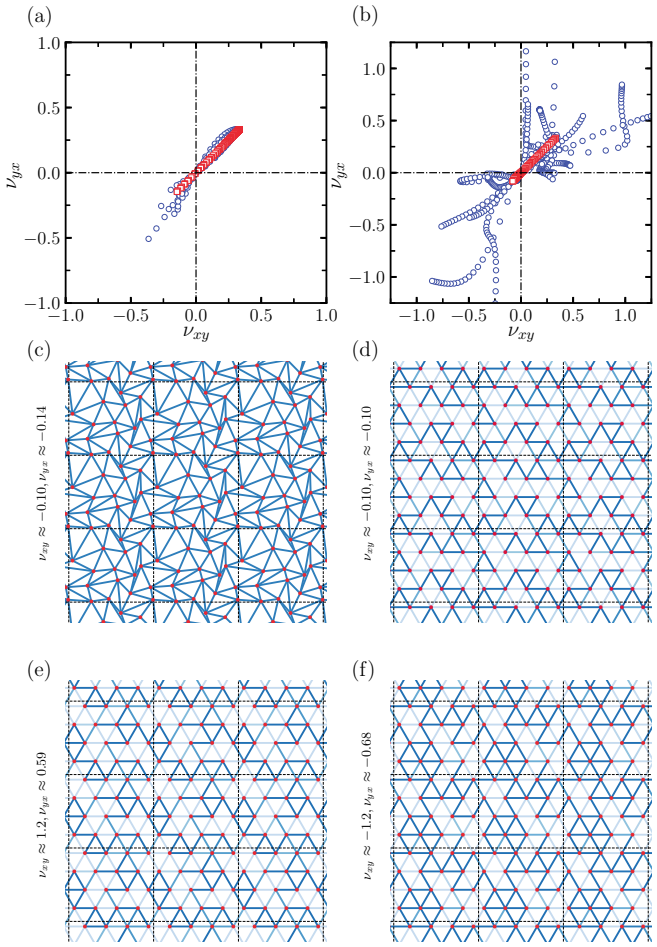

FIG. 7. Elastic properties of small systems evolved from the triangular lattice and examples of mechanical metamaterials using such small systems as building blocks. (a) and (b) show the correlation between ν_{xy} and ν_{yx} as defined in the text with the change of the magnitude of the node displacement η and the parameter α, respectively. In (a), $\alpha = 0$ and all bonds have identical stiffness. The data are collected for various η. In (b), there is no real lattice distortion ($\eta = 0$). We perform a virtual lattice distortion with $\eta^* = 0.2$ and collect data by varying α. Circles and squares are for $N = 16$ and 16384, respectively. Horizontal (vertical) dot-dashed lines label $\nu_{yx} = 0$ ($\nu_{xy} = 0$). Apparently, $\nu_{xy} \approx \nu_{yx}$ for $N = 16\,384$ systems in both cases, which does not hold when $N = 16$, especially when α is varied in (b). [(c)–(f)] Examples of periodic metamaterials with $N = 16$ systems being building blocks. The dashed lines are boundaries of the building blocks. The values of ν_{xy} and ν_{yx} are given on the left side of each example. The gray scale of the bonds in (d), (e), and (f) is the same as shown in Fig. 4(a).

we are still able to use them as building blocks to generate auxetic networks.

Figures 7(a) and 7(b) show ν_{xy} against ν_{yx} for the $N = 16$ and 16384 networks with the variation of η ($\alpha = 0$) and α ($\eta = 0$ and $\eta^* = 0.2$), respectively, where ν_{yx} (ν_{xy}) is the Poisson's ratio calculated by applying compression in the x (y) direction. For the $N = 16\,384$ systems which tend to be isotropic when disorder is sufficiently large, $\nu_{xy} \approx \nu_{yx}$. In contrast, the $N = 16$ systems show strong anisotropy with a large dispersion of the data points in the (ν_{xy}, ν_{yx}) plane,

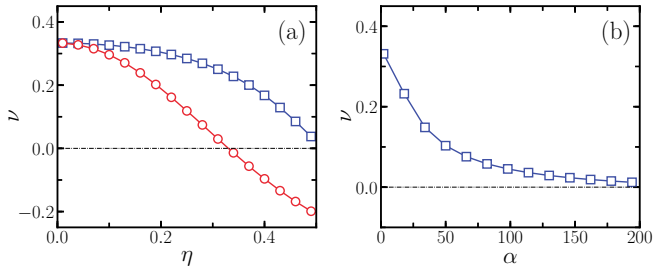

FIG. 8. Evolution of the Poisson's ratio with disorder induced by the lattice distortion for the three-dimensional FCC lattice. (a) and (b) show Poisson's ratio ν calculated in the ⟨100⟩ direction against the magnitude of the node displacement η and the parameter α for the $N = 16384$ systems, respectively. In (a), squares and circles are for $\alpha = 0$ and 5, respectively. The virtual distortion for (b) is $\eta^* = 0.1$. The solid lines are guides for the eye. The horizontal dot-dashed lines label $\nu = 0$.

when α is varied in the perfect triangular lattice geometry following a virtual lattice distortion, as shown in Fig. 7(b). The anisotropy is weaker when there is no bond stiffness disorder and only η is varied, as shown in Fig. 7(a). For the $N = 16$ systems, there are still realizations with negative Poisson's ratio, which can thus be building blocks to form periodic auxetic materials.

Figure 7(b) also shows that due to the anisotropy there are certain realizations of the $N = 16$ systems exhibiting a directional Poisson's ratio exceeding the limits of isotropic materials. It is known that auxetic materials with $\nu < -1$ can be obtained by taking advantage of anisotropy [8,18]. In comparison, the metamaterials with $\nu > 1$ which are densified upon stretch are rare [13]. Using small systems as building blocks, we broaden the range of the Poisson's ratio that can be achieved.

In Figs. 7(c)–7(f), we show examples of periodic metamaterials with different Poisson's ratios. The advantage of our approach beyond previous ones is that we are able to easily realize various metamaterials just by manipulating disorder, especially the bond stiffness disorder. And we gain the freedom to adjust the values of the Poisson's ratio with lots of realizations to use. In contrast, previous approaches only have limited choices with particular structures. Our approach will definitely facilitate the design of auxetic materials and metamaterials with $\nu > 1$.

G. Auxeticity in three-dimensional networks

Up to now, we have shown the realization of auxeticity in two dimensions. In three dimensions, face centered cubic (FCC) and hexagonal close-packed (HCP) lattices are stackings of the triangular lattice. It is thus straightforward to realize auxeticity in these close-packed cubic lattices by simply stacking auxetic triangular lattices. However, this auxeticity is still directional. We wish to see whether the same manipulations of disorder done for two-dimensional systems can lead to isotropic auxeticity as well in three dimensions.

Here we take the FCC lattice as the example. As shown in Fig. 8(a), auxetic networks may still be obtained by distorting the FCC lattice with a sufficiently large η, but here η_c will be

above 0.5, the upper limit of the distortion that we set to avoid the possible crossing of bonds. The adjustment of the bond stiffness also pushes auxetic networks to occur at a smaller lattice distortion. Figure 8(b) shows that by introducing the bond stiffness disorder according to the virtual lattice distortion we dramatically decrease the Poisson's ratio with the increase of α. In contrast to the two-dimensional triangular lattice, the Poisson's ratio here does not become negative, while just decaying almost to zero. This may be due to a weaker correlation between bond length and elastic moduli than two-dimensional systems. A more subtle manipulation of the bond stiffness disorder may be required to boost the decay of the Poisson's ratio in order to obtain isotropic auxeticity in cubic lattice geometries.

IV. DISCUSSION

Taking advantage of disorder, we propose a new approach to tune elastic moduli of spring networks and obtain auxetic materials, without the need of designing building blocks with specific geometries favorable to auxeticity or breaking the topology. The key is that the disorder must be introduced in some correlated way following the (virtual) network distortion.

An important finding of our work is that auxetic materials can be obtained by just adjusting the bond stiffness of spring networks. As an example, we successfully turn the triangular lattice into auxetic, even though the lattice does not meet the conditions required by previous approaches to realize auxeticity. Of course, due to the bond stiffness disorder and the spatial heterogeneity of local elasticity, the structure of the resultant system is effectively different from the initial one, although the lattice site locations and topology remain unchanged. Therefore there are still structural origins of the auxeticity discussed here, which would be rather complicated due to the presence of disorder and require more follow-up studies.

Both our approach (except for the pure lattice distortion with $\alpha = 0$) and the pruning-bond approach [22–27] introduced in Sec. I play with individual bonds, which may to some extent perform similar functions. Instead of pruning bonds [22], if we try to make bonds with large g_i stiffer and bonds with large b_i softer (g_i and b_i are defined in Sec. III B), we may be able to effectively decrease the Poisson's ratio of unstressed jammed solids. On the other hand, after the lattice is distorted, we may also decrease the Poisson's ratio by pruning short bonds, with a special attention to maintaining the network rigidity. However, note that the precondition for the pruning-bond approach to take effect is that *the disorder is already present*. As discussed in Sec. I, it is ineffective on perfect lattices, because all bonds are identical. In this sense, our approach is more general and should have broader applications. Moreover, maintaining the topology frees us from the worry of losing rigidity. Compared with g_i and b_i, the bond length is much easier to measure, which makes our approach more experimentally accessible.

Here we only show results of manipulating close-packed lattices. Our major findings should be general and valid to other types of spring networks. For instance, we have successfully turned unstressed and disordered networks extracted from jammed solids into auxetic by applying the bond stiffness disorder following the virtual network distortion, which will be discussed elsewhere. More work is certainly required to figure out whether and how network symmetry and topology may affect the results, especially for some special ones like kagome lattice [41] which already exhibit extraordinary elastic properties [42–44]. Note that here we do not take into account the bond angle rigidity, which is important to stabilize some hypostatic lattices, e.g., honeycomb. It is also interesting to know whether there is any analogous way to manipulate bond angle rigidity disorder and hence the Poisson's ratio.

Moreover, in addition to the formation of auxetic materials, the $\alpha < 0$ curve in Fig. 3(c) indicates that the Poisson's ratio of networks with apparent structural disorder can be tuned to higher values. We expect that adjusting the bond stiffness of unstressed and disordered solids by means of network distortion may induce extraordinary mechanical and vibrational properties distinct from normal disordered solids. This may reveal new aspects of disordered solids and help us further understand how different types of disorder affect each other to determine special properties of disordered solids.

ACKNOWLEDGMENTS

We thank D. Frenkel, T. Lubensky, P. Tan, and F. Ye for instructive discussions. This work was supported by the National Natural Science Foundation of China Grants No. 11734014 and No. 11574278. We also thank the Supercomputing Center of University of Science and Technology of China for the computer time.

[1] L. D. Landau and E. M. Lifshitz, *Theory of Elasticity* (Pergamon, Oxford, 1970).
[2] R. Lakes, Foam structures with a negative poisson's ratio, Science **235**, 1038 (1987).
[3] G. B. Gardner, D. Venkataraman, J. S. Moore, and S. Lee, Spontaneous assembly of a hinged coordination network, Nature **374**, 792 (1995).
[4] K. E. Evans, M. A. Nkansah, I. J. Hutchinson, and S. C. Rogers, Molecular network design, Nature (London) **353**, 124 (1991).
[5] G. N. Greaves, A. L. Greer, R. S. Lakes, and T. Rouxel, Poisson's ratio and modern materials, Nat. Mater. **10**, 823 (2011).
[6] U. D. Larsen, O. Sigmund, and S. Bouwstra, Design and fabrication of compliant micromechanisms and structures with negative Poisson's ratio, J. Microelectromechanical Syst. **6**, 99 (1997).
[7] J.-W. Jiang and H. S. Park, Negative poisson's ratio in single-layer black phosphorus, Nat. Commun. **5**, 4727 (2014).
[8] M. Schenk and S. D. Guest, Geometry of Miura-folded metamaterials, Proc. Natl. Acad. Sci. USA **110**, 3276 (2013).
[9] Z. Y. Wei, Z. V. Guo, L. Dudte, H. Y. Liang, and L. Mahadevan, Geometric Mechanics of Periodic Pleated Origami, Phys. Rev. Lett. **110**, 215501 (2013).

[10] B. Florijn, C. Coulais, and M. van Hecke, Programmable Mechanical Metamaterials, Phys. Rev. Lett. **113**, 175503 (2014).
[11] J. N. Grima and K. E. Evans, Auxetic behavior from rotating squares, J. Mater. Sci. Lett. **19**, 1563 (2000).
[12] J. N. Grima, S. Winczewski, L. Mizzi, M. C. Grech, R. Cauchi, R. Gatt, D. Attard, K. W. Wojciechowski, and J. Rybicki, Tailoring graphene to achieve negative poisson's ratio properties, Adv. Mater. **27**, 1455 (2014).
[13] L. J. Hall, V. R. Coluci, D. S. Galvão, M. E. Kozlov, M. Zhang, S. O. Dantas, and R. H. Baughman, Sign Change of Poisson's Ratio for Carbon Nanotube Sheets, Science **320**, 504 (2008).
[14] V. R. Coluci, L. J. Hall, M. E. Kozlov, M. Zhang, S. O. Dantas, D. S. Galvão, and R. H. Baughman, Modeling the auxetic transition for carbon nanotube sheets, Phys. Rev. B **78**, 115408 (2008).
[15] R. H. Baughman and D. S. Galvão, Crystalline networks with unusual predicted mechanical and thermal properties, Nature (London) **365**, 735 (1993).
[16] C. Huang and L. Chen, Negative poisson's ratio in modern functional materials, Adv. Mater. **28**, 8079 (2016).
[17] J. N. Grima and R. Caruana-Gauci, Materials that push back, Nat. Mater. **11**, 565 (2012).
[18] H. M. A. Kolken and A. A. Zadpoor, Auxetic mechanical metamaterials, RSC Adv. **7**, 5111 (2017).
[19] R. H. Baughman, J. M. Shacklette, A. A. Zakhidov, and S. Stafström, Negative poisson's ratios as a common feature of cubic metals, Nature (London) **392**, 362 (1998).
[20] U. Schärer and P. Wachter, Negative elastic constants in intermediate valent $Sm_xLa_{1-x}S$, Solid State Commun. **96**, 497 (1995).
[21] N. R. Keskar and J. R. Chelikowsky, Anomalous elastic behavior in crystalline silica, Phys. Rev. B **48**, 16227 (1993).
[22] C. P. Goodrich, A. J. Liu, and S. R. Nagel, The Principle of Independent Bond-Level Response: Tuning by Pruning to Exploit Disorder for Global Behavior, Phys. Rev. Lett. **114**, 225501 (2015).
[23] D. R. Reid, N. Pashine, J. M. Wozniak, H. M. Jaeger, A. J. Liu, S. R. Nagel, and J. J. de Pablo, Auxetic metamaterials from disordered networks, Proc. Natl. Acad. Sci. USA **115**, E1384 (2018).
[24] D. Hexner, A. J. Liu, and S. R. Nagel, Role of local response in manipulating the elastic properties of disordered solids by bond removal, Soft Matter **14**, 312 (2018).
[25] J. W. Rocks, N. Pashine, I. Bischofberger, C. P. Goodrich, A. J. Liu, and S. R. Nagel, Designing allostery-inspired response in mechanical networks, Proc. Natl. Acad. Sci. USA **114**, 2520 (2017).
[26] L. Yan, R. Ravasio, C. Brito, and M. Wyart, Architecture and coevolution of allosteric materials., Proc. Natl. Acad. Sci. USA **114**, 2526 (2017).
[27] V. F. Hagh and M. F. Thorpe, Disordered auxetic networks with no reentrant polygons, Phys. Rev. B **98**, 100101(R) (2018).
[28] E. Bitzek, P. Koskinen, F. Gähler, M. Moseler, and P. Gumbsch, Structural Relaxation Made Simple, Phys. Rev. Lett. **97**, 170201 (2006).
[29] C. S. O'Hern, L. E. Silbert, A. J. Liu, and S. R. Nagel, Jamming at zero temperature and zero applied stress: The epitome of disorder, Phys. Rev. E **68**, 011306 (2003).
[30] L. E. Silbert, A. J. Liu, and S. R. Nagel, Vibrations and Diverging Length Scales Near the Unjamming Transition, Phys. Rev. Lett. **95**, 098301 (2005).
[31] M. Wyart, L. E. Silbert, S. R. Nagel, and T. A. Witten, Effects of compression on the vibrational modes of marginally jammed solids, Phys. Rev. E **72**, 051306 (2005).
[32] M. Wyart, S. R. Nagel, and T. A. Witten, Geometric origin of excess low-frequency vibrational modes in weakly connected amorphous solids, Europhys. Lett. **72**, 486 (2005).
[33] X. Mao, N. Xu, and T. C. Lubensky, Soft Modes and Elasticity of Nearly Isostatic Lattices: Randomness and Dissipation, Phys. Rev. Lett. **104**, 085504 (2010).
[34] Y. Nie, H. Tong, J. Liu, M. Zu, and N. Xu, Role of disorder in determining the vibrational properties of mass-spring networks, Front. Phys. **12**, 126301 (2017).
[35] H. Tong, P. Tan, and N. Xu, From crystals to disordered crystals: A hidden order-disorder transition, Sci. Rep. **5**, 15378 (2015).
[36] X. Wang, W. Zheng, L. Wang, and N. Xu, Disordered Solids without Well-Defined Transverse Phonons: The Nature of Hard-Sphere Glasses, Phys. Rev. Lett. **114**, 035502 (2015).
[37] A. Zaccone and E. M. Terentjev, Short-range correlations control the G/K and Poisson ratios of amorphous solids and metallic glasses, J. Appl. Phys. **115**, 033510 (2014).
[38] W. G. Ellenbroek, Z. Zeravcic, W. van Saarloos, and M. van Hecke, Non-affine response: Jammed packings vs. spring networks, Europhys. Lett. **87**, 34004 (2009).
[39] C. Maloney and A. Lemaître, Subextensive Scaling in the Athermal, Quasistatic Limit of Amorphous Matter in Plastic Shear Flow, Phys. Rev. Lett. **93**, 016001 (2004).
[40] C. E. Maloney and A. Lemaître, Amorphous systems in athermal, quasistatic shear, Phys. Rev. E **74**, 016118 (2006).
[41] M. Mekata, Kagome: The story of the basketweave lattice, Phys. Today **56**(2), 12 (2003).
[42] K. Sun, A. Souslov, X. Mao, and T. C. Lubensky, Surface phonons, elastic response, and conformal invariance in twisted kagome lattices, Proc. Natl. Acad. Sci. USA **109**, 12369 (2012).
[43] X. Mao, Q. Chen, and S. Granick, Entropy favours open colloidal lattices, Nat. Mater. **12**, 217 (2013).
[44] X. Mao and T. C. Lubensky, Maxwell lattices and topological mechanics, Annu. Rev. Condens. Matter Phys. **9**, 413 (2018).